

1 **Synchronous intensification and warming of Antarctic Bottom Water**
2 **outflow from the Weddell Gyre**

3

4

5 Michael P. Meredith¹, Arnold L. Gordon², Alberto C. Naveira Garabato³, E. Povl

6 Abrahamsen¹, Bruce A. Huber², Loïc Jullion³ and Hugh J. Venables¹

7

8

9 ¹ *British Antarctic Survey, High Cross, Madingley Road, Cambridge, CB3 0ET, U.K.*

10 ² *Lamont-Doherty Earth Observatory of Columbia University, 61 Route 9W,*

11 *Palisades, New York, 10964-8000, U.S.A.*

12 ³ *National Oceanography Centre Southampton, European Way, Southampton, SO14*

13 *7ZH, U.K.*

14

14 **Abstract**

15

16 Antarctic Bottom Water (AABW), the densest water in the global overturning
17 circulation, has warmed in recent decades, most notably in the Atlantic. Time series
18 recorded within the boundary currents immediately upstream and downstream of the
19 most significant outflow of AABW from the Weddell Sea indicate that raised outflow
20 temperatures are synchronous with stronger boundary current flows. These changes
21 occur rapidly in response to changes in wind forcing, suggesting that barotropic
22 dynamics and the response of the bottom Ekman layer are significant. The observed
23 synchronicity indicates that the previously-detected weakening of the export of the
24 colder forms of AABW from the Weddell Sea need not be associated with a reduction
25 in the total flux of AABW exported via this route. These points need careful
26 consideration when attributing the observed AABW warming in the Atlantic, and
27 when determining its contribution to global heat budgets and sea level rise.

28

28 **Introduction**

29

30 The Weddell Sea hosts the production of Weddell Sea Deep Water (WSDW), the
31 main contributor to the cold Antarctic Bottom Water (AABW) that permeates much
32 of the global ocean abyss [Orsi *et al.*, 1999]. While AABW in the low-latitude
33 Atlantic is often taken as the ensemble of waters colder than 2 °C, WSDW itself has
34 potential temperatures between ~0 and -0.7 °C, and forms directly through intense air-
35 sea-ice interaction at the periphery of the Weddell Sea, as well as via upwelling of
36 Weddell Sea Bottom Water [e.g. Gordon *et al.*, 2001; Meredith *et al.*, 2000]. It
37 circulates cyclonically within the boundary currents of the Weddell gyre before being
38 exported across and around the South Scotia Ridge (Figure 1), with Orkney Passage
39 (OP) being the most direct throughflow for WSDW to enter the Atlantic overturning
40 circulation [Naveira Garabato *et al.*, 2002; Schodlok *et al.*, 2002]. Around one quarter
41 of all dense Antarctic-derived waters colder than 0 °C flow through OP, after which
42 they flow north and east across the Scotia Sea [Meredith *et al.*, 2001; Meredith *et al.*,
43 2008] and westward in a boundary current toward Drake Passage. They do not,
44 however, penetrate significantly into the Pacific [Nowlin and Zenk, 1988].

45

46 In recent decades, AABW has warmed significantly in many regions, most strongly in
47 the Atlantic [e.g. Meredith *et al.*, 2008; Zenk and Morozov, 2007]. This warming has
48 reached the North Atlantic, where it was interpreted as a slowing in the meridional
49 overturning of Antarctic-derived waters [Johnson *et al.*, 2008]. The warming has a
50 magnitude of potential significance for the global heat budget and calculations of sea
51 level rise [Purkey and Johnson, 2010].

52

53 There have been a number of investigations of variability of deep and bottom waters
54 in the Weddell Sea [e.g. *Fahrbach et al.*, 2004; *Schröder et al.*, 2002], however the
55 absence of clearly-defined trends in WSDW properties has focused attention on
56 processes that might control its characteristics as it exits the Weddell Sea. Based on
57 hydrographic data from the Scotia Sea, *Meredith et al.* [2001; 2008] proposed that
58 changes in cyclonic wind-forcing over the Weddell gyre could impact on the
59 steepness of isopycnal surfaces in the northern Weddell Sea, and hence on the
60 temperature of the coldest water that crosses the South Scotia Ridge. *Jullion et al.*
61 [2010] used a more comprehensive data set, and found a surprisingly short lag (just a
62 few months) between changes in wind stress curl over the Weddell gyre and
63 temperatures of WSDW exported through OP. If such processes were relevant on
64 decadal timescales, the observed strengthening of winds over the Southern Ocean
65 [e.g. *Thompson and Solomon*, 2002] could plausibly be responsible for the warming
66 of AABW in the Atlantic, due to the coldest classes of WSDW being progressively
67 restricted from crossing the South Scotia Ridge [*Meredith et al.*, 2008]. Here we
68 present observational evidence and dynamical arguments concerning local controls on
69 both the temperature and strength of the outflow of WSDW from the Weddell Sea,
70 and discuss the implications for large-scale water mass properties and ocean climate.

71

72 **Data sources**

73

74 Data were obtained from two *in situ* instruments, one in the northern Weddell Sea,
75 and one in the southern Scotia Sea (Figure 1). The former was the uppermost
76 instrument on mooring M2 of the Consortium on the Ocean's Role in Climate: Abrupt
77 Climate Changes Studies (CORC-ARCHES) program [e.g. *Gordon et al.*, 2010]. M2

78 was deployed at 62°38'S, 43°15'W in water depth ~3059 m, with the uppermost
79 instrument (a Sea-Bird SBE37 Microcat temperature/conductivity recorder) located
80 2580 m below the surface. The latter was the Multi-Year Recording Tide Level
81 Equipment [MYRTLE; *Spencer and Foden*, 1996], a long-duration bottom pressure
82 recorder deployed on the seabed at 60°03'S, 47°10'W (~2350 m depth) between late
83 1999 and late 2003. The MYRTLE temperature sensor was not calibrated for absolute
84 temperature, so only anomalies are used; these are precise to 0.001 °C. We also use
85 wind stress data from the ERA-Interim reanalysis
86 (<http://www.ecmwf.int/products/data/archive/descriptions/ei/index.html>).

87

88 **Results**

89

90 MYRTLE and M2 temperature anomalies correlate well for much of their length with
91 a lag of 120 days (M2 leading MYRTLE; Figure 2a), specifically during 2002 and
92 2003 for which the correlation at this lag (0.6) is significant at the 95% level. (Note
93 that MYRTLE is scaled by 0.7 in Figure 2. M2 data were obtained from the
94 uppermost instrument on a long mooring, whilst MYRTLE data were obtained with a
95 bottom lander and hence came from closer to the core of the bottom-intensified
96 boundary current). For a path length between the two sites of ~500 km (Figure 1), this
97 120 day lag equates to a flow speed of ~4.8 cm s⁻¹, somewhat less than the 7.9 cm s⁻¹
98 quoted by *Nowlin and Zenk* [1988] for boundary current speeds at ~2000 m depth to
99 the west of MYRTLE. However, considering the full period of data overlap suggests
100 that ~4.8 cm s⁻¹ may underestimate the true long-term mean. Specifically, during
101 2001, the lag of 120 days shows poor agreement between MYRTLE and M2 (Figure
102 2a), whereas 60 days yields significantly better agreement. (For this section of data, a

103 120 day lag gives a correlation of 0.2, compared with 0.55 for 60 days). This shorter
104 lag equates to a flow speed of $\sim 9.6 \text{ cm s}^{-1}$. For comparison, long-term current meter
105 records at M2 give a mean speed of 8.3 cm s^{-1} [Gordon *et al.*, 2010], though no such
106 data are available from M2 for 2001 itself.

107

108 Significantly, temperature anomalies during the period of shorter-lag correlation
109 (2001) were higher than those during the period of longer-lag correlation (2002 and
110 2003) (Figure 2). The length of the transition between these two periods is hard to
111 quantify precisely, but cannot exceed a few months (Figure 2).

112

113 The depths of M2 and MYRTLE data were different, at $\sim 2580 \text{ m}$ and 2350 m
114 respectively. Recent multi-beam echo sounder data (not shown) give a sill depth of
115 $\sim 3600 \text{ m}$ for the narrowest part of OP, and depths ~ 2500 to $\sim 3350 \text{ m}$ along a shallower
116 ridge immediately upstream. This indicates that WSDW passing the top of M2 can
117 cross the South Scotia Ridge relatively unimpeded, although it will sink and mix as it
118 does so. That the M2 and MYRTLE temperature anomalies show strong similarities
119 indicates vertical coherence in temperature, given this sinking and mixing and the
120 shallower location of MYRTLE compared with M2.

121

122 **Discussion**

123

124 Coincident with the period of shorter-lag correlation between MYRTLE and M2,
125 zonal wind stress along the South Scotia Ridge was anomalously strong during the
126 latter part of 2001 (Figure 2f, 2g, 3), with the end of this period matching closely the
127 transition to the longer-lag relationship between MYRTLE and M2 (Figure 2a, 2c).

128 This echoes the timescale of just a few months for the response of WSDW to winds
129 found previously [Jullion *et al.*, 2010]. Given the rapid and synchronous response of
130 WSDW temperature and speed to changes in forcing, we suggest that the key
131 mechanism involved is the response of the bottom Ekman layer to barotropic changes
132 in the strength of the deep boundary current that flows along the sloping topography
133 of the northern Weddell Sea.

134

135 As described by *Garrett et al.* [1993] and *Brink and Lentz* [2010] amongst others, any
136 along-slope geostrophic flow over sloping topography gives rise to a bottom Ekman
137 layer that displaces isopycnals away from their equilibrium depth and that is
138 ultimately arrested by buoyancy forces. The arrest time for a downwelling-favorable
139 along-slope geostrophic flow such as the deep boundary current in the northern
140 Weddell Sea (or, in other words, the time scale on which a change in the along-slope
141 geostrophic velocity is balanced by an adjustment of the bottom Ekman layer) is
142 estimated by $t_{arrest} = 0.5 c_d^{-1} N^{-1} S^{-3/2}$, where c_d is the frictional bottom drag
143 coefficient, N is the buoyancy frequency, and $S = N^2 f^{-2} \sin^2 \theta$ is the Burger number
144 based on the bottom slope ($\tan \theta$) and the inertial frequency f [*Garrett et al.*, 1993].
145 Using values typical for the northern Weddell Sea boundary current ($c_d \approx 2.5 \times 10^{-3}$, N
146 $\approx 10^{-3} \text{ s}^{-1}$, $f \approx 10^{-4} \text{ s}^{-1}$, $\theta \approx 2^\circ$, $S \approx 0.12$), we obtain $t_{arrest} \sim 54$ days, broadly consistent
147 with the baroclinic adjustment time scale suggested by the observations.

148

149 That the bottom Ekman velocity anomaly associated with the adjustment process is
150 sufficiently large to produce the observed change in WSDW temperature may be
151 shown using the relationship between the Ekman layer velocity v_{Ek} and the along-
152 slope geostrophic speed U_g , i.e. $v_{Ek} = 2.5 c_d^{1/2} U_g$, where the reduction in the Ekman

153 flow resulting from buoyancy effects has been neglected for simplicity [e.g., *Brink*
154 *and Lentz*, 2010]. An approximate halving of the boundary current speed from ~ 0.1 m
155 s^{-1} in the last 9 months of 2001 to ~ 0.05 m s^{-1} thereafter is suggested by observations,
156 implying a reduction in v_{Ek} of $\sim 6 \times 10^{-3}$ m s^{-1} . If such a reduced Ekman flow acted
157 adiabatically on a topographic slope $\theta \approx 2^\circ$ over a time scale $t_{arrest} \sim 54$ days, the
158 implied uplift of isopycnals would be ~ 900 m, well in excess of the ~ 100 m suggested
159 by observations. In practice, this isopycnal displacement is a gross overestimate, due
160 to the assumption that the Ekman flow on the slope proceeds unimpeded by buoyancy
161 forces, and serves simply to quantitatively illustrate the plausibility of the proposed
162 mechanism of baroclinic adjustment.

163

164 Other potential mechanisms do not seem able to explain our rapid synchronous
165 changes in WSDW outflow temperature and strength. For example, at typical rates of
166 $O(10 \text{ m } y^{-1})$, local forcing by anomalous surface Ekman pumping / suction would take
167 several years to displace isopycnals vertically by ~ 100 m, the amount required to
168 change the temperature of the coldest WSDW exported by the $\sim 0.04^\circ\text{C}$ observed [e.g.
169 *Gordon et al.*, 2001]. Further, changes in the formation properties of WSDW such as
170 have been inferred [e.g. *Fahrbach et al.*, 2004] are unlikely to have the rapid
171 timescale that characterize the shifts in both temperature and flow speed that we have
172 observed, nor are they likely to have such a short-period relationship to changes in
173 local atmospheric forcing.

174

175 We hypothesized previously that large-scale cyclonic wind forcing over the extent of
176 the Weddell gyre may control the northward export of WSDW across the South
177 Scotia Ridge [*Meredith et al.*, 2001; 2008]. Our new observations do not preclude

178 this, however it is important to note that classical gyre-wide baroclinic adjustment at
179 high latitudes is characterized by time scales of decades [e.g., *Anderson and Gill*,
180 1975], which would result in a significantly longer response timescale than that
181 observed here. We thus suggest that any comparatively slow changes in outflow due
182 to changes in large-scale cyclonic forcing will have more rapid (and potentially
183 larger) changes superposed on them due to barotropic and Ekman processes near the
184 outflow itself.

185

186 **Conclusions**

187

188 AABW in the Atlantic is warming rapidly, and determining the causes of this is
189 important if the implications for global heat budgets and sea level rise are to be
190 correctly quantified and understood. If, as has been suggested previously, the cause of
191 this warming were a reduction in the northward export of the colder classes of
192 WSDW (as opposed to the same volume being exported with higher temperatures)
193 such calculations will need to account for this to avoid regional overestimates of heat
194 content and thermal expansion. Our findings support the notion of the colder classes
195 of WSDW being progressively restrained from leaving from the Weddell Sea,
196 however the synchronous nature of the temperature and export speed of WSDW in
197 response to changing winds adds significant further complexity. Specifically, it now
198 seems possible that a wind-induced reduction in the export of the colder classes of
199 AABW into the Atlantic overturning circulation can be associated with an increase in
200 the export of the warmer classes. The balance between these factors in controlling the
201 overall export flux is presently unknown.

202

203 Similar to the AABW in the North Atlantic [*Johnson et al.*, 2008], bottom waters in
204 the North Pacific have also warmed recently [*Fukasawa et al.*, 2003]. The rapid
205 timescale of this warming (order of four decades) was likely accomplished by a fast
206 teleconnection facilitated by internal Rossby and Kelvin waves, which have the action
207 of slowing the deep currents that transport AABW northwards. If true also in the
208 Atlantic, with the perturbations that generated the wave teleconnection being changes
209 in the WSDW outflow of the type described here, the superposition of such fast wave-
210 mediated signals upon slower advective changes would generate significant
211 complexity, and make attribution of measured deep ocean climate change even more
212 challenging. This is compounded by the fact that the outflow processes outlined here
213 are not represented in current climate-scale ocean models.

214

215 The changes in WSDW observed here were caused by changes in winds that project
216 strongly onto the pattern of the Southern Annular Mode (SAM), consistent with
217 *Jullion et al.* [2010]. The SAM has moved to a higher-index state in recent decades,
218 associated with anthropogenic forcing from ozone depletion and/or greenhouse gases,
219 resulting in stronger winds over the Southern Ocean [*Marshall, 2003; Thompson and*
220 *Solomon, 2002*]. To the extent that the mechanisms described here are relevant on
221 decadal timescales, this carries the implication that anthropogenic processes may be
222 significant in the abyssal warming along the length of the Atlantic. If the winds over
223 the Southern Ocean continue to strengthen in future years and decades (either via
224 there being a stronger mean, or more frequent events such as that seen in 2001), this
225 could result in warmer classes of WSDW being supplied more efficiently to the lower
226 limb of the global overturning circulation. To detect and correctly attribute such
227 changes, a system capable of monitoring both properties and fluxes is required.

228 Accordingly, we will deploy shortly a comprehensive mooring array in the narrowest
229 part of OP. Sustaining this for several decades will be difficult, but is required to meet
230 the challenges outlined here.

231

232

233 **Acknowledgements**

234 We thank Peter Foden, Steve Mack, Bob Spencer and Ian Vassie for their work with
235 MYRTLE. ACNG and LJ were supported by the Natural Environment Research
236 Council (NERC), via an Advanced Research Fellowship (NE/C517633/1) and the
237 ANDREX project (NE/E01366X/1). M2 research was funded under the Cooperative
238 Institute for Climate Applications Research award NA08OAR4320754 from the
239 National Oceanic and Atmospheric Administration (NOAA), U.S. Department of
240 Commerce. The statements, findings, conclusions, and recommendations are those of
241 the authors and do not necessarily reflect the views of NERC, NOAA or the
242 Department of Commerce. This is Lamont Doherty contribution number 7426, and a
243 contribution of the British Antarctic Survey's Polar Oceans program.

244

244 **References**

- 245 Anderson, D. L. T., and A. E. Gill (1975), Spin-up of a stratified ocean, with
246 applications to upwelling, *Deep-Sea Research*, 22(9), 583-596.
- 247 Brink, K. H., and S. J. Lentz (2010), Buoyancy arrest and bottom Ekman transport,
248 Part I: Steady Flow, *Journal of Physical Oceanography*, 40, 621-635.
- 249 Fahrback, E., et al. (2004), Decadal-scale variations of water mass properties in
250 the deep Weddell Sea, *Ocean Dynamics*, 54(77-91).
- 251 Fukasawa, M., et al. (2003), Bottom water warming in the North Pacific Ocean,
252 *Nature*, 427, 825-827.
- 253 Garrett, C., et al. (1993), Boundary mixing and arrested Ekman layers: rotating
254 stratified flow near a sloping boundary, *Annual Reviews of Fluid Mechanics*, 25,
255 291-323.
- 256 Gordon, A. L., et al. (2001), Export of Weddell Sea Deep and Bottom Water,
257 *Journal of Geophysical Research*, 106(C5), 9005-9017.
- 258 Gordon, A. L., et al. (2010), A seasonal cycle in the export of bottom water from
259 the Weddell Sea, *Nature Geoscience*, 3, 10.1038/ngeo916.
- 260 Johnson, G. C., et al. (2008), Reduced Antarctic meridional overturning circulation
261 reaches the North Atlantic Ocean, *Geophysical Research Letters*, 35(L22601),
262 doi:10.1029/2008GL035619.
- 263 Jullion, L., et al. (2010), Wind-controlled export of Antarctic Bottom Water from
264 the Weddell Sea, *Geophysical Research Letters*, 37(L09609).
- 265 Marshall, G. J. (2003), Trends in the Southern Annular Mode from Observations
266 and Reanalyses, *Journal of Climate*, 16, 4134-4143.
- 267 Meredith, M. P., et al. (2000), On the sources of Weddell Gyre Antarctic Bottom
268 Water, *Journal of Geophysical Research*, 105(C1), 1093-1104.

269 Meredith, M. P., et al. (2001), Deep and Bottom Waters of the Eastern Scotia Sea:
270 Rapid Changes in Properties and Circulation, *Journal of Physical Oceanography*,
271 31(8), 2157-2168.

272 Meredith, M. P., et al. (2008), Evolution of the Deep and Bottom Waters of the
273 Scotia Sea, Southern Ocean, 1995-2005, *Journal of Climate*, 21(13), 3327-3343.

274 Naveira Garabato, A. C., et al. (2002), Modification and pathways of Southern
275 Ocean Deep Waters in the Scotia Sea, *Deep-Sea Research I*, 49, 681-705.

276 Nowlin, W. D., and W. Zenk (1988), Westward bottom currents along the margin
277 of the South Shetland Island Arc, *Deep Sea Research*, 35, 269-301.

278 Orsi, A. H., et al. (1999), Circulation, mixing, and production of Antarctic Bottom
279 Water, *Progress in Oceanography*, 43(1), 55-109.

280 Purkey, S. G., and G. C. Johnson (2010), Antarctic Bottom Water Warming
281 Between the 1990s and the 2000s: Contributions to Global Heat and Sea Level
282 Rise Budgets, *Journal of Climate*, *accepted*.

283 Schodlok, M. P., et al. (2002), On the transport, variability and origin of dense
284 water masses crossing the South Scotia Ridge, *Deep Sea Research II*, 49, 4807-
285 4825.

286 Schröder, M., et al. (2002), On the near-bottom variability in the northwestern
287 Weddell Sea, *Deep Sea Research II*, 49, 4767-4790.

288 Spencer, R., and P. R. Foden (1996), Data from the deep ocean via releasable data
289 capsules, *Sea Technology*, 37(2), 10-12.

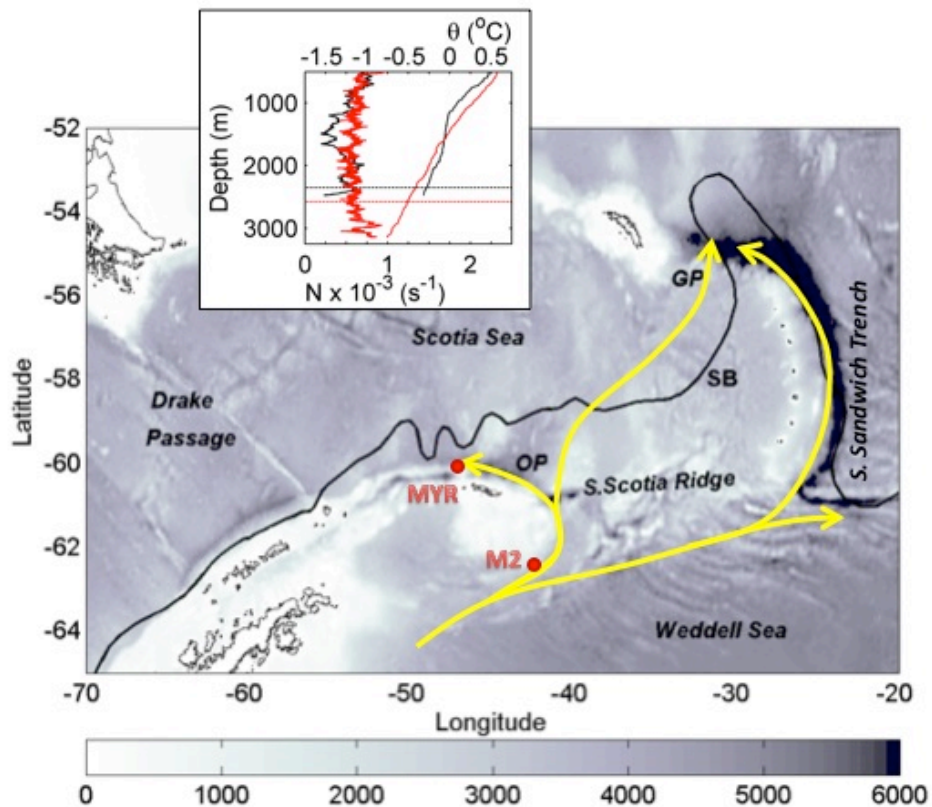
290 Thompson, D. W. J., and S. Solomon (2002), Interpretation of recent Southern
291 Hemisphere climate change, *Science*, 296, 895-899.

292 Zenk, W., and E. Morozov (2007), Decadal warming of the coldest Antarctic
293 Bottom Water flow through the Vema Channel, *Geophysical Research Letters*,
294 34(L14607), 10.1029/2007GL030340.

295

296

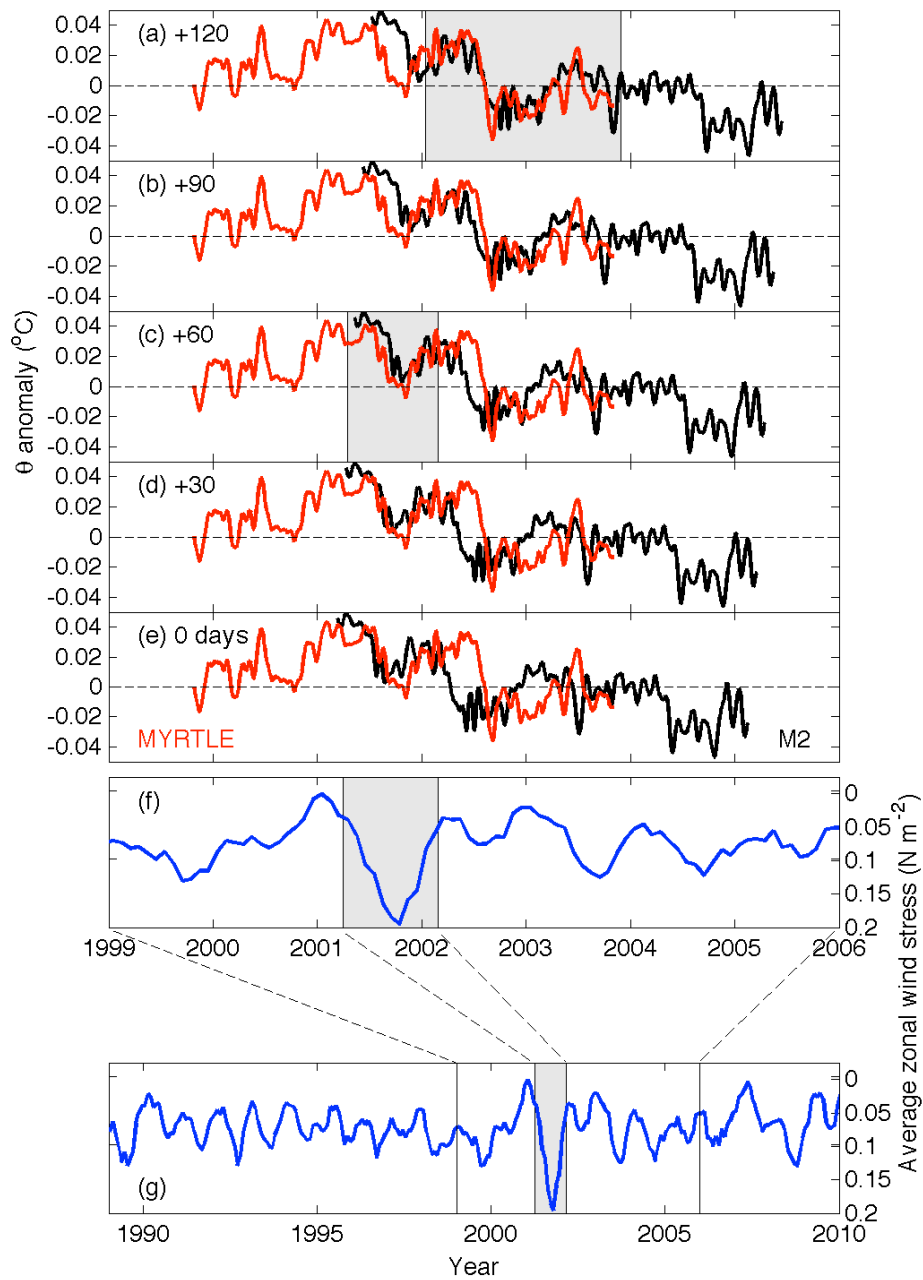
297



298

299 **Figure 1.** Locations of M2 and MYRTLE in the northern Weddell Sea and southern
 300 Scotia Sea (red dots). Yellow arrows depict the primary flow paths of WSDW through
 301 the region: Orkney Passage (OP) on the South Scotia Ridge and Georgia Passage
 302 (GP) at the northeastern Scotia Sea are key throughflows. The Southern Boundary
 303 (SB) of the Antarctic Circumpolar Current is marked. Background shading is depth
 304 (m). Inset shows typical potential temperature and buoyancy frequency profiles from
 305 the location of M2 (red) and close to the site of MYRTLE (black). The depths of the
 306 MYRTLE and M2 temperature sensors used here are marked.

307



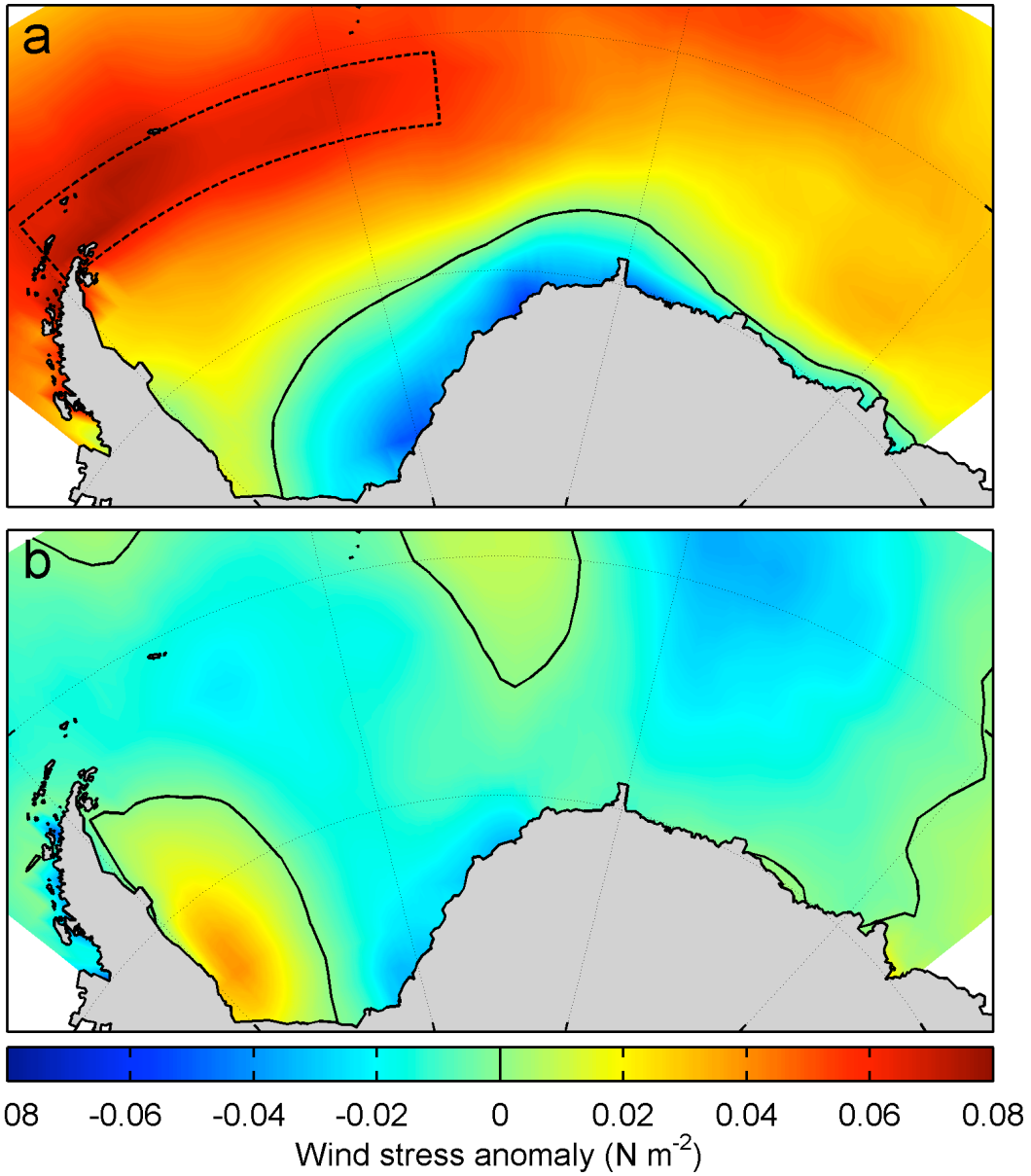
307

308 **Figure 2(a-e).** Temperature anomaly at M2 (black) and MYRTLE (red), for lags of 0
 309 to 120 days. MYRTLE and M2 correlate well at 120 days lag, except for the first ~9
 310 months, during which a 60 day lag yields the highest correlation (shaded boxes in (a)
 311 and (c) highlight these periods). **(f)** Zonal wind stress averaged over the northern
 312 Weddell Sea (area of averaging marked in Figure 3a). Curve is a five-point running
 313 average of monthly-mean values, plotted inverted. Shaded box is as per Figure 2c,

314 during which period wind forcing reached a record-length extreme. (g) as for (f), but

315 for the full length of ERA-Interim.

316



316

317 **Figure 3 (a)** Zonal and **(b)** meridional wind stress anomalies respectively, for the last

318 9 months of 2001. The zero N m^{-2} contour is plotted. Note the strong anomaly in

319 eastward wind stress at the northern edge of the Weddell Sea during this period.